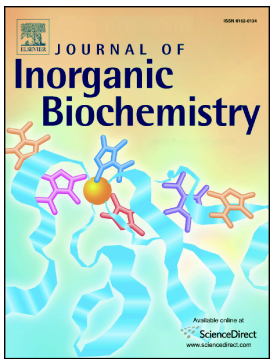

Comparative solution and structural studies of half-sandwich rhodium and ruthenium complexes bearing curcumin and acetylacetone

János P. Mészáros, Jelena M. Poljarevic, G. Tamás Gál, Nóra V. May, Gabriella Spengler, Éva A. Enyedy

PII: S0162-0134(18)30751-7
DOI: https://doi.org/10.1016/j.jinorgbio.2019.02.015
Reference: JIB 10660

To appear in: *Journal of Inorganic Biochemistry*

Received date: 20 December 2018
Revised date: 15 February 2019
Accepted date: 26 February 2019

Please cite this article as: J.P. Mészáros, J.M. Poljarevic, G.T. Gál, et al., Comparative solution and structural studies of half-sandwich rhodium and ruthenium complexes bearing curcumin and acetylacetone, Journal of Inorganic Biochemistry, https://doi.org/10.1016/j.jinorgbio.2019.02.015

Comparative solution and structural studies of half-sandwich rhodium and ruthenium complexes bearing curcumin and acetylacetone

János P. Mészáros,[a] Jelena M. Poljarevic,[a,b] G. Tamás Gál,[c] Nóra V. May,[c] Gabriella Spengler,[d] Éva A. Enyedy[a]*

[a] Department of Inorganic and Analytical Chemistry, Interdisciplinary Excellence Centre, University of Szeged, Dóm tér 7, H-6720 Szeged, Hungary

[b] University of Belgrade - Faculty of Chemistry, Studentski trg 12-16, 11000 Belgrade, Serbia

[c] Research Centre for Natural Sciences Hungarian Academy of Sciences, Magyar tudósok körútja 2, H-1117 Budapest, Hungary

[d] Department of Medical Microbiology and Immunobiology, University of Szeged, Dóm tér 10, H-6720 Szeged, Hungary

Keywords: Curcumin; Solution stability; X-ray crystal structures; Half-sandwich complexes; Cytotoxicity

* Corresponding author.

E-mail address: enyedy@chem.u-szeged.hu (É.A. Enyedy).

ABSTRACT

Half-sandwich organometallic complexes of curcumin are extensively investigated as anticancer compounds. Speciation studies were performed to explore the solution stability of curcumin complexes formed with $[Rh(\eta^5\text{-}C_5Me_5)(H_2O)_3]^{2+}$. Acetylacetone (Hacac), as the simplest β-diketone ligand bearing (O,O) donor set, was involved for comparison and its Ru(η^6-*p*-cymene), Ru(η^6-toluene) complexes were also studied. ^{1}H NMR, UV-visible and pH-potentiometric titrations revealed a clear trend of stability constants of the acac complexes: Ru(η^6-p-cymene) > Ru(η^6-toluene) > Rh(η^5-C_5Me_5). Despite this order, the highest extent of complex formation is seen for the Rh(η^5-C_5Me_5) complexes at pH 7.4. Formation constant of $[Rh(\eta^5\text{-}C_5Me_5)(H_2curcumin)(H_2O)]^+$ reveals similar solution stability to that of the acac complex. Additionally, structures of two complexes were determined by X-ray crystallography. The *in vitro* cytotoxicity of curcumin was not improved by the complexation with these organometallic cations.

1. Introduction

The field of anticancer drug research is governed by two main factors: efficacy and selectivity. *Cisplatin* (cis-diammine-dichloridoplatinum(II)) and its derivatives are the leading compounds of the metal-based chemotherapeutics [1,2]. They possess high cytotoxicity, although their use is limited by acquired resistance and side effects caused by the low selectivity [1]. The development of novel compounds based on platinum group metal ions is an attractive alternative. The Ru(III)-containing *trans*-[tetrachlorido(DMSO)(imidazole) ruthenate(III)] (*NAMI-A*) [3] and *trans*-[tetrachloridobis(1*H*-indazole)ruthenate(III)] (*KP1339/IT-139*) are considered as the most promising candidates, and the latter complex already demonstrated remarkable anticancer activity in a phase I clinical trial [4]. Ru(III) is assumed to be activated by reduction giving the impetus for the development of Ru(II) compounds. A novel Ru(II) compound, [ruthenium(II)(4,4'-dimethyl-2,2'-bipyridine)2-(2-(2',2":5",2‴-terthiophene)-imidazo[4,5-f][1,10-phenanthroline)]Cl_2 (*TLD-1433*, *NCT03053635*) has entered clinical trials in 2016 as a photodynamic agent [6]. In the half-sandwich arrangement Ru(II) is protected from hydrolysis and oxidation by the coordination of an aromatic ligand, and faster ligand-exchange processes can be observed [7,8]. The assumed mechanism of action of this type of complexes is often connected to their ability to bind to biomolecules and/or to their redox properties. [Ru(η^6-arene)(PTA)Cl_2] (RAPTA) complexes show *in vivo* activity combined with low toxicity [9]. The group of [Ru(η^6-arene)(1,2-ethylenediamine)Cl]$^+$ (RAED) compounds developed by Sadler *et al.* also exhibits significant anticancer activity [10,11].

The congener Os(II), Rh(III) and Ir(III) compounds are paid somewhat less attention, although some of their half-sandwich complexes have as high cytotoxicity as cisplatin [7,12]. The physico-chemical properties of the [Ru/Os(η^6-arene)(X,Y)(Z)] and [Rh/Ir(η^5-arenyl)(X,Y)(Z)] complexes can be optimized by changing the building blocks, *e.g.* the arene (or arenyl) ring, the bidentate (X,Y) ligand or the co-ligand (Z).

Compounds bearing (O,O) donor set are often used as ligands like cyclobutane dicarboxylate in carboplatin, or oxalate in oxaliplatin [1]. These ligands are found in carbo-RAPTA and oxali-RAPTA as well [9]. β-diketones are one of the oldest groups of (O,O) ligands used in analytical and synthetic approaches and a plenty of their half-sandwich complexes were synthesized [13]. The simplest β-diketone molecule is acetylacetone (Hacac, Chart 1), however there are numerous natural compounds containing this motif such as dibenzoylmethane (*Glycyrrhiza glabra*) [14], gingerols (*Zingiber officinale*) or curcumin

(*Curcuma longa*) [15,16]. The most attractive property of them is their low toxicity against healthy cells and they possess intrinsic anticancer properties [15,16].

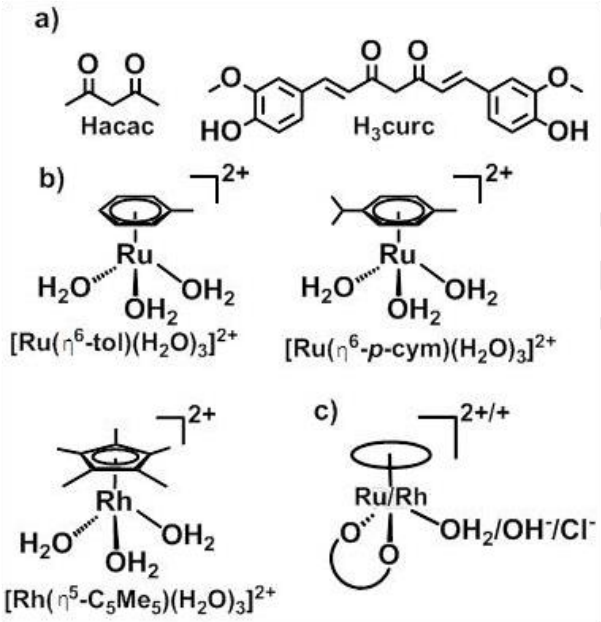

Chart 1. a) Chemical structures of the investigated (O,O) bidentate ligands: acetylacetone (Hacac) and curcumin (H_3curc); and b) organometallic half-sandwich triaqua cations. c) General chemical structure of the mono complexes formed with (O,O) bidentate ligands.

Curcumin (H_3curc, Chart 1) and its derivatives alone or in combination with metal ions have been reported to show significant antitumor activity and induce paraptotic effects on cancer cells [17]. Curcumin is able to overcome P-glycoprotein mediated multidrug resistance in human cancer cells via the inhibition of this transporter [15,16]. However curcumin has very low solubility in water, it is photosensitive and may completely hydrolyse under strongly basic conditions [18-20] These features make the solution equilibrium studies fairly difficult. The insufficient pharmacokinetic properties of curcumin can be overcome by binding to a protein or a metal ion [19-21]. A plethora of curcumin metal complexes was synthesized in which the ligand could be stabilized. These complexes are potential photosensitizers for photodynamic therapy in cancer treatment [21]. Its half-sandwich Ru(II) complex was tested against human cancer cell lines showing moderate activity (IC_{50} = 13.98-62.33 μM) [22]. The $[Rh(\eta^5\text{-}C_5Me_5)(H_2curc)(H_2O)]^+$ complex is considered as a delivery system of curcumin since its cytotoxicity is similar to that of the ligand itself [23]. The combination of PTA and curcumin in half-sandwich organo-metallic complexes could enhance the bioactivity [13].

Despite the high number of organometallic complexes formed with curcumin and its derivatives reported in the literature, the solution stability of this type of compounds was not characterized and compared to analogous species. As the metal complexes are generally considered as prodrugs and can undergo ligand exchange processes in biofluids, information about their solution speciation is needed for understanding of their transformation processes. Therefore solution stability, aquation (replacement of the chlorido leaving group by a water molecule) and deprotonation processes were already studied in our former works in case of half-sandwich complexes containing (pentamethylcyclopentadienyl)-rhodium(III) (Rh(η^5-C_5Me_5)), (*p*-cymene)ruthenium(II) (Ru(η^6-*p*-cym)) and (toluene)ruthenium(II) (Ru(η^6-tol)) as the organometallic fragment and various bidentate ligands [24-29]. Herein our aim was to investigate the complex formation of curcumin (H_3curc) and acetylacetone (Hacac) with $[Rh(\eta^5\text{-}C_5Me_5)(H_2O)_3]^{2+}$, $[Ru(\eta^6\text{-}p\text{-cym})(H_2O)_3]^{2+}$ and $[Ru(\eta^6\text{-tol})(H_2O)_3]^{2+}$ organometallic cations (Chart 1) using pH-potentiometry, UV-visible (UV-Vis) and ^{1}H NMR spectroscopy. Interaction of the acac complexes with human serum albumin (HSA) and cell culture medium components was characterized by spectrofluorometry and ^{1}H NMR spectroscopy to reveal the possible transformation processes. Effect of the complexation on the *in vitro* cytotoxicity of curcumin was also tested in multidrug resistant Colo 320/MDR-LRP human colonic adenocarcinoma cell lines.

2. Results and discussion

2.1. Hydrolysis of the organometallic cations and proton dissociation processes of ligands

For the complete description of the equilibrium processes in the organometallic cation – ligand systems the hydrolysis constants of the metal ions and the proton dissociation constants of the ligands are needed. The hydrolytic behaviour of the organometallic $[Ru(\eta^6\text{-}p\text{-cym})(H_2O)_3]^{2+}$ and $[Ru(\eta^6\text{-tol})(H_2O)_3]^{2+}$ cations has been already studied by Buglyó *et al*. in the presence and in the absence of chloride ions [30]. The fast hydrolysis of the aquated organoruthenium cations yields the species $[(Ru(\eta^6\text{-arene}))_2(\mu^2\text{-}OH)_3]^+$ that becomes predominant at pH > ~4.5 (tol) and ~5 (*p*-cym). When 0.2 M KCl was used as the background electrolyte, like in our studies, formation of various chlorido and mixed chlorido/hydroxido species as intermediates was found in addition to the major hydrolysis product $[(Ru(\eta^6\text{-arene}))_2(\mu^2\text{-}OH)_3]^+$ [31].

Table 1. Proton dissociation constants (pK_a of the studied ligands and stability constants (log K [ML]) of organometallic acatylacetonate complexes and overall stability constant (log β [MLH_2]) of $[Rh(\eta^5\text{-}C_5Me_5)(H_2curc)(H_2O)]^+$, p$K_a$ [ML], pH_{max}, $\%_{ML,max}$ and $pM^*_{7.4}$ values determined by various methods, and H_2O/Cl^- exchange constants (log K' [ML]) for $[Rh(\eta^5\text{-}C_5Me_5)(acac)(H_2O/Cl)]^{+/0}$ {T = 25 °C; I = 0.2 M (KCl)}.[a]

	Acetylacetone			**Curcumin**	
	Ru(η^6-tol)	**Ru(η^6-*p*-cym)[b]**	**Rh(η^5-C_5Me_5)**	**Rh(η^5-C_5Me_5)**	
pK_a (HL)[c]		8.76 ± 0.01		pK_a (H_3L)[d]	7.72 ± 0.06
				pK_a (H_2L)[d]	9.54 ± 0.01
				pK_a (HL)[d]	10.32 ± 0.01
log K [ML]	7.93 ± 0.09[c] 8.09 ± 0.04[e]	8.56	6.44 ± 0.01[c] 6.48 ± 0.01[e]	log β [MLH_2]	25.76 ± 0.04[f]
pK_a [ML]	9.32 ± 0.03[e]	—	—		
pH_{max}[g]	5.32	5.72	8.08	pH_{max}[g]	7.84
$\%_{ML,max}$[g]	8	35	44	$\%_{ML,max}$[g]	48
$pM^*_{7.4}$[h]	5.31	5.35	5.45	$pM^*_{7.4}$[h]	5.54
log K' (H_2O/Cl^-)[i]	—	—	1.11 ± 0.01		

[a] The overall stability constants of organometallic cation's hydrolysis products: log β $[(Ru(\eta^6\text{-tol}))_2(\mu^2\text{-}OH)_2]^{2+}$ = –6.50, log β $[(Ru(\eta^6\text{-tol}))_2(\mu^2\text{-}OH)_3]^+$ = –10.56; log β $[(Ru(\eta^6\text{-}p\text{-cym}))_2(\mu^2\text{-}OH)_2]^{2+}$ = –7.12, log β $[(Ru(\eta^6\text{-}p\text{-cym}))_2(\mu^2\text{-}OH)_3]^+$ = –11.88; log β $[(Rh(\eta^5\text{-}C_5Me_5))_2(\mu^2\text{-}OH)_2]^{2+}$ = –11.12, log β $[(Rh(\eta^5\text{-}C_5Me_5))_2(\mu^2\text{-}OH)_3]^+$ = –19.01 at I = 0.20 M (KCl) taken from Refs. [24,30].
[b] Taken from Ref. [35].
[c] Determined by pH-potentiometric titrations.
[d] Determined by UV-Vis titrations at pH = 6.0-11.6.
[e] Determined by ^{1}H NMR titrations.
[f] Constant for $[Rh(\eta^5\text{-}C_5Me_5)(H_2curc)(H_2O)]^+$ determined by UV-Vis spectrometry at pH = 6.8, c(M)/c(L) = 0.0-8.6.
[g] Calculated for systems containing c(M) = c(L) = 5 μM. pH_{max} is the pH at which the extent of the formation of the metal complexes is the highest and $\%_{ML,max}$ is the highest fraction of ML under this condition. pM* = -log($[M]^{2+}$+2$[M_2(\mu^2\text{-}OH)_2]^{2+}$+2$[M_2(\mu^2\text{-}OH)_3]^+$).
[h] Calculated for systems containing c(M) = c(L) = 5 μM and at pH = 7.4.
[i] Determined by UV-Vis spectrometry: c(Cl^-) = 0.0-0.3 M, pH = 7.3.

Stability constants for the hydrolysis products of $[Rh(\eta^5\text{-}C_5Me_5)(H_2O)_3]^{2+}$ have been reported by our group, namely for $[(Rh(\eta^5\text{-}C_5Me_5))_2(\mu^2\text{-}OH)_2(H_2O)_2]^{2+}$ and $[(Rh(\eta^5\text{-}C_5Me_5))_2(\mu^2\text{-}OH)_3]^{+}$ dinuclear species [24]. Notably, the hydrolysis of $Rh(\eta^5\text{-}C_5Me_5)(H_2O)_3]^{2+}$ starts at higher pH compared with the $Ru(\eta^6$-arene) species.

Proton dissociation process of acetylacetone (Hacac) is well-known in the literature and the pK_a constant determined by pH-potentiometry in this work (Table 1) is in a good agreement with the reported values [32]. Acetylacetone has two tautomeric forms, namely keto and enol, which are distinguishable in the ^{1}H NMR spectra due to the slow exchange processes on the NMR time-scale (Figure S1). The reported enol/keto equilibrium constant is log $K_{enol/keto}$ = 0.21 [32], and a similar constant was determined based on our measurements (log $K_{enol/keto}$ = 0.23 ± 0.02). As a consequence the keto form predominates in aqueous solutions in the whole pH range studied.

Curcumin has the same β-diketonato group as Hacac, although the proton dissociation occurs not merely in this moiety since the two phenolic hydroxyl groups have dissociable protons as well. Only few data can be found for the pK_a values of these moieties in the literature most probably as a consequence of the low water solubility and light-induced decomposition of this compound [33]. Therefore, the proton dissociation constants of curcumin were determined by UV-Vis spectroscopy in a 95% water/5% ethanol mixture using low concentration (5 μM) and individual samples kept in dark (see Figure S2). By the deconvolution of the recorded UV-Vis spectra three pK_a values were calculated (Table 1). Presumably the β-diketonato group has the lowest pK_a, which is actually lower than the same group's constant in the Hacac molecule. The two higher constants belong to the overlapping deprotonation of the two 2-methoxyphenolic groups.

2.2. Complex formation equilibria of acac with $[Rh(\eta^5\text{-}C_5Me_5)(H_2O)_3]^{2+}$ and $[Ru(\eta^6\text{-}tol)(H_2O)_3]^{2+}$

As studies on the solution speciation of curcumin complexes are aggravated owing to the insufficient water solubility and light-sensitivity, acetylacetone, possessing a similar coordination mode, served as a water soluble model ligand. The solution speciation of the $[Ru(\eta^6\text{-}p\text{-cym})(H_2O)_3]^{2+}$ – acac system was already studied by Bíró *et al.*, and they determined the log *K* [ML] formation constant for the mono complex (log *K* [ML] = 8.56, *I* = 0.2 M KCl) [35]. (M denotes the organometallic triaqua cation

in which the aqua ligand are partly replaced by the chlorido ligands and the donor atoms of the ligands.) Fernández *et al*. determined the pK_a [ML] constant (9.41) for the deprotonation of the coordinated water, although a chloride-free medium was applied (I = 0.1 M $NaClO_4$) [36].

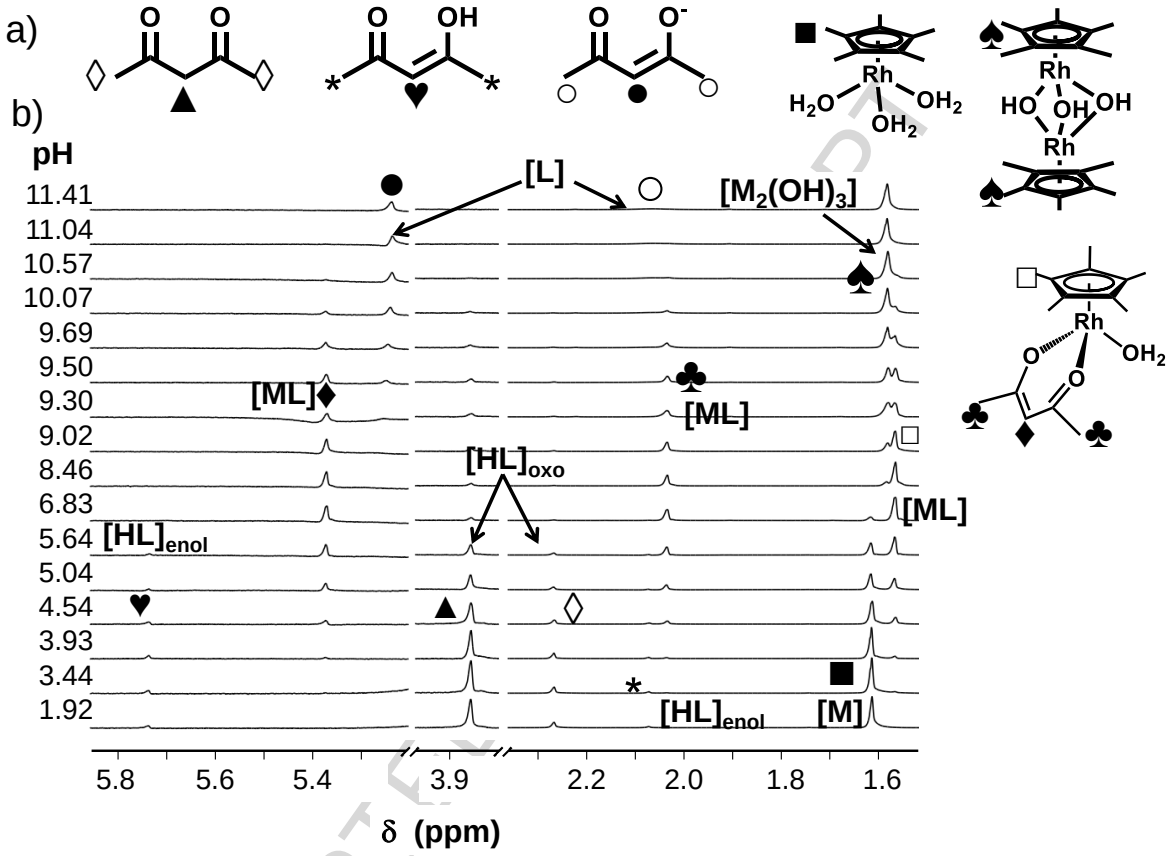

Figure 1. a) Chemical structures of compounds present in the $[Rh(\eta^5\text{-}C_5Me_5)(H_2O)_3]^{2+}$– acac system. b) ^{1}H NMR spectra of $[Rh(\eta^5\text{-}C_5Me_5)(H_2O)_3]^{2+}$– acac system recorded at pH = 1.9-11.4. Peak assignation is shown on the structures of a). (M denotes the organometallic half-sandwich triaqua cation. Notably the aqua ligand is partly displaced by chloride.) {c(acac) = 2.0 mM; c([$Rh(\eta^5\text{-}C_5Me_5)(H_2O)_3]^{2+}$) = 2.1 mM; solvent: 90% H_2O / 10% D_2O; T = 25.0 °C; I = 0.2 M (KCl)}

Stability constants of acetylacetonato complexes formed with the other two organometallic cations were determined by the combined use of pH-potentiometric and ^{1}H NMR titrations in the presence of 0.2 M chloride ions. It is worth mentioning that complex formation was found to be fairly fast in all cases. In the speciation model formation of mono complexes such as [ML] and [ML(OH)] was used based on single crystal X-ray diffraction results (*vide infra*) and the findings on analogous complexes of other bidentate (O,O) ligands investigated previously [24,25,35]. Figure 1 shows ^{1}H

NMR spectra recorded for the $[Rh(\eta^5\text{-}C_5Me_5)(H_2O)_3]^{2+}$ – acac system in the pH range from 1.9 to 11.4. At acidic pH range (pH < 3.5) only the peaks of the free organometallic ion and free ligand (in both the keto and enol forms) can be identified. In the pH range 3.5-10.0 a new set of signals appears which is related to the formation of complex $[Rh(\eta^5\text{-}C_5Me_5)(L)(H_2O)]^+$ that predominates at physiological pH (in which H_2O is partly replaced by Cl^-).

On the other hand in case of the $[Ru(\eta^6\text{-tol})(H_2O)_3]^{2+}$ – acac system, formation of mixed hydroxido complex $[Ru(\eta^6\text{-tol})(acac)(OH)]$ can be also detected at pH > 8 (Figure S3,a). The aqua and hydroxido complexes are in equilibrium with high exchange rates that cannot be resolved in the NMR time scale. Thus the peaks of the mono complex are high-field shifted as the pH is increased and draw a sigmoid curve (Figure S3,c). This phenomenon allows the determination of pK_a [ML] constant from the change of the chemical shifts (Table 1). As the signals assigned to free and bound acac ligand as well as to the unbound and bound organometallic fragment appear separately in the ^{1}H NMR spectra the integrated peak areas could be converted to molar fractions. Based on the molar fractions at the different pH values stability constants (log *K* [ML]) were computed for the $[Ru(\eta^6\text{-tol})(H_2O)_3]^{2+}$ – acac and $[Rh(\eta^5\text{-}C_5Me_5)(H_2O)_3]^{2+}$ – acac systems (Table 1). They are in a fairly good agreement with data determined by pH-potentiometry. In order to compare the stability constants of acac complexes to those of other simple (O,O) donor ligands, log *K* [ML] and pK_a [ML] values were determined for deferiprone and maltol complexes of $Ru(\eta^6\text{-tol})$ by pH-potentiometry. (Constants were already reported for deferiprone and maltol complexes of $Rh(\eta^5\text{-}C_5Me_5)$ and $Ru(\eta^6\text{-cym})$ [24,25,35].) The log *K* [ML] for the deferiprone $Ru(\eta^6\text{-tol})$ complex is 11.74 ± 0.08 and pK_a [ML] is 9.34 ± 0.09. While in the $[Ru(\eta^6\text{-tol})(H_2O)_3]^{2+}$ – maltol system only one constant, log *K* [ML] = 8.97 ± 0.01 was determined. The trend of the log *K* [ML] constants of the acac species is the following: $[Ru(\eta^6\text{-}p\text{-cym})(acac)(H_2O)]^+$ > $[Ru(\eta^6\text{-tol})(acac)(H_2O)]^+$ >> $[Rh(\eta^5\text{-}C_5Me_5)(acac)(H_2O)]^+$, which is the same trend as seen with other (O,O) donor ligands such as maltol [24,35] and deferiprone [25,35]. To compare the apparent solution stability of the acac complexes pM* values were computed and plotted against the pH (Figure 2). pM* value, which is defined as the negative logarithm of the equilibrium concentrations of the unbound metal ion (in all forms: triaqua cation and μ-hydroxido dinuclear species) under the given conditions (pH, total concentrations of the ligand

and metal ion). Notably, pM was introduced by Raymond *et al*. [37] to compare the relative affinities of ligands towards a given metal ion. Therefore, a higher pM* value reflects the stronger metal binding ability of the ligand. Due to the stronger tendency of $[Ru(\eta^6\text{-arene})(H_2O)_3]^{2+}$ cations to undergo hydrolysis at physiological pH compared to that of $[Rh(\eta^5\text{-}C_5Me_5)(H_2O)_3]^{2+}$ [24,30], the highest extent of complex formation is found in the $[Rh(\eta^5\text{-}C_5Me_5)(H_2O)_3]^{2+}$ – acac system under the same conditions (Figure 2). Table 1 also contains the % [ML] at these pH values and the $pM^*_{7.4}$ values.

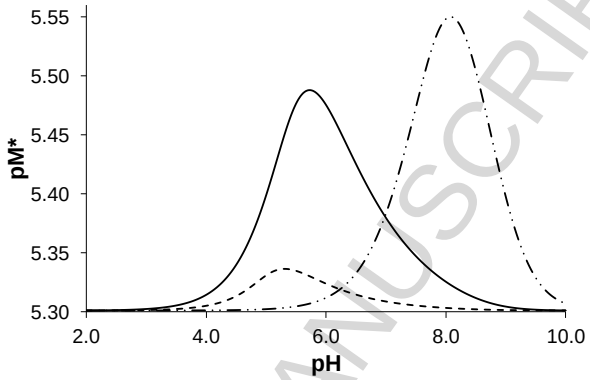

Figure 2. Calculated pM*-curves obtained for the organometallic cation – acac systems plotted against the pH. M = $[Rh(\eta^5\text{-}C_5Me_5)(H_2O)_3]^{2+}$ (-···-···-); $[Ru(\eta^6\text{-}p\text{-cym})(H_2O)_3]^{2+}$ (—) [35]; $[Ru(\eta^6\text{-tol})(H_2O)_3]^{2+}$ (- - -). {c(acac) = c(M) = 5 μM; T = 25.0 °C; I = 0.2 M (KCl)}

2.3. Complex formation equilibrium of curcumin with $[Rh(\eta^5\text{-}C_5Me_5)(H_2O)_3]^{2+}$

Concentrations necessary for pH-potentiometric and ^{1}H NMR titrations cannot be reached in pure water in case of curcumin. As curcumin has very intensive colour, UV-Vis spectrophotometric titrations were performed in 95% water/5% ethanol mixture. Stock solution was prepared before the measurements by dissolving curcumin in ethanol and then stored in the dark. In ethanol the hydrolysis of curcumin does not occur [18]. In case of $[Ru(\eta^6\text{-}p\text{-cym})(H_2O)_3]^{2+}$ and $[Ru(\eta^6\text{-tol})(H_2O)_3]^{2+}$ the spectral changes showed that their curcumin complexes have even lower solubility than curcumin itself leading to precipitation. Therefore, stability constants for the $Ru(\eta^6$-arene) complexes could not be obtained under these conditions. In order to determine the stability constant for the $[Rh(\eta^5\text{-}C_5Me_5)(H_2curc)(H_2O)]^+$ complex known amounts of the organometallic cation were added to the ligand and UV-Vis spectra were recorded while the pH was kept constant (pH 6.8) using phosphate buffer (Figure S4.). During the titration organorhodium cation was added to curcumin at a maximum of 9-

fold excess. Formation of a $[Rh(\eta^5\text{-}C_5Me_5)(H_2curc)(H_2O)]^+$ complex is assumed as the deprotonation of the non-coordinating 2-methoxyphenolic groups under these conditions is not probable based on the pK_a values of curcumin. Since the determination of the stability constants of the organoruthenium complexes of curcumin failed, it is an interesting point to check how good binding model is acac for curcumin. The stability constants determined for the complexes of acac and curcumin cannot be compared directly due to the different deprotonation processes of the ligands. Thus, concentration distribution curves for the $[Rh(\eta^5\text{-}C_5Me_5)(H_2O)_3]^{2+}$ – acac and $[Rh(\eta^5\text{-}C_5Me_5)(H_2O)_3]^{2+}$ – curcumin systems are represented in Figure 3. It can be concluded that the curves run rather close to each other for both systems, however the curcumin complex shows a slightly higher stability. Therefore, acac is not a perfect but an adequate binding model ligand for the solution speciation studies of curcumin complexes.

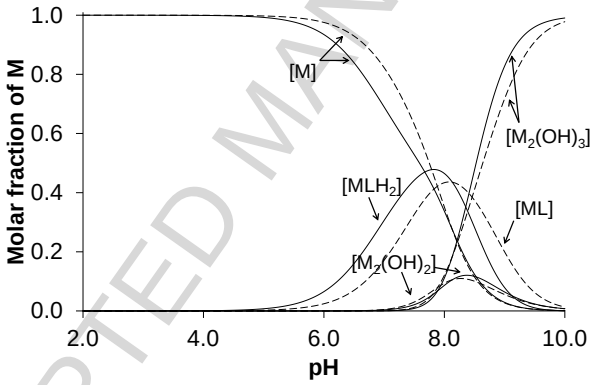

Figure 3. Calculated concentration distribution curves of $[Rh(\eta^5\text{-}C_5Me_5)(H_2O)_3]^{2+}$ – acac (dashed lines) and $[Rh(\eta^5\text{-}C_5Me_5)(H_2O)_3]^{2+}$ – curcumin (solid lines) systems based on the stability constants from Table 1. {c(M) = c(acac) = c(curcumin) = 5 μM; T = 25.0 °C; I = 0.2 M (KCl)}

The solution stability of the studied half-sandwich $Rh(\eta^5\text{-}C_5Me_5)$ complexes of acac and curcumin was compared to that of (O,O) donor bearing ligands such as maltol [24], allomaltol [24] or deferiprone [25] via the calculation of pM* values at various pH values (Figure 4). It can be concluded that curcumin and acac form complexes with lower stability than the other ligands with 5-membered chelate ring.

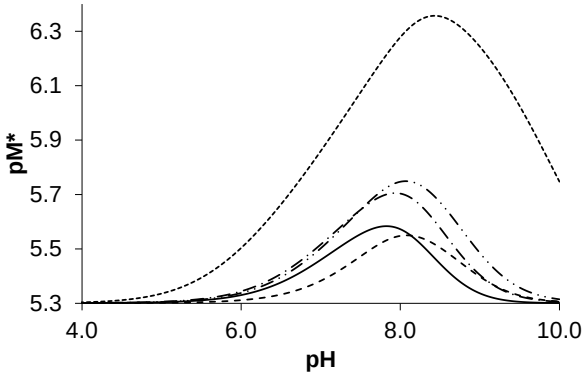

Figure 4. Calculated pM*-curves of $[Rh(\eta^5\text{-}C_5Me_5)(H_2O)_3]^{2+}$ – (O,O) bidentate ligand systems plotted against the pH. Notations for the various ligands: acac (- - -); curcumin (–); allomaltol [24] (-·-·-); maltol [24] (-···-); deferiprone [25] (---). pM* = –log([M] + 2[$M_2(OH)_3$] + 2[$M_2(OH)_2$]), where M denotes the triaqua organometallic cation. Notably the coordinated H_2O is partly replaced by Cl^- in the complexes in the presence of the chloride ions. {*c*(M) = *c*(L) = 5 mM; *T* = 25.0 °C; *I* = 0.2 M (KCl)}

2.4. Structural studies on organometallic Rh(III) and Ru(II) complexes

Single crystals were obtained for metal complexes $Ru(\eta^6\text{-tol})(acac)Cl]$ (**1**) and $[Rh(\eta^5\text{-}C_5Me_5)(H_2curc)Cl] \times 2MeOH$ (**2**) by the reaction of the ligands deprotonated by sodium methoxide and the corresponding organometallic dimer precursors. The dimeric ruthenium precursor $[Ru(\eta^6\text{-tol})(\mu^2\text{-Cl})Cl]_2$ was prepared according to literature procedures by the reaction of $RuCl_3 \times 3H_2O$ with 1-methyl-1,4-cyclohexadiene [38], while $[Rh(\eta^5\text{-}C_5Me_5)(\mu^2\text{-Cl})Cl]_2$ is commercially available. The mixtures of the ligands and the precursors were refluxed for 4 h and then the solvent was removed. The complex was dissolved and extracted with CH_2Cl_2. Single crystals of the acac complex were grown in concentrated methanolic solutions. In the case of the $[Rh(\eta^5\text{-}C_5Me_5)(H_2curc)(Cl)]$ complex crystals were obtained from a mixture of $MeOH/CH_2Cl_2$.

The $[Ru(\eta^6\text{-tol})(acac)(Cl)]$ complex was crystallized without any remaining solvent molecule, while $Rh(\eta^5\text{-}C_5Me_5)(H_2curc)(Cl)]$ crystallized with two methanol molecules in the asymmetric unit. The ORTEP representation of the complexes showing the atom and ring labels is depicted in Figure 5. The complexes crystallized in the monoclinic and in the orthorombic crystal system, in space group $P2_{1/c}$ and Pbcn, respectively. Selected bond distances and angles are collected in Table 2, structure refinement and crystal data are shown in Table S1. The geometry of the complexes are

pseudo-tetrahedral: they show the so-called three-legged 'piano-stool' geometry similarly to the previously determined complexes with bidentate (O,O) and Cl^- donor groups [22,24,25,36,39]. Additional information about hydrogen bonds and packing arrangements in crystal **1** is collected in Table S2 and Figs. S5 and S6.

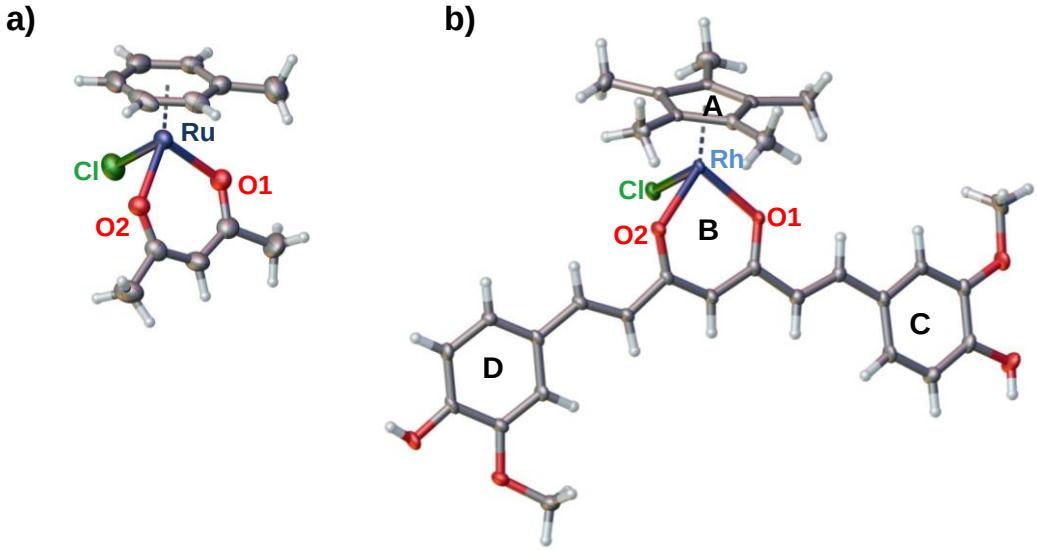

Figure 5. a) Molecular structures of [Ru(η^6-tol)(acac)(Cl)] (**1**) and b) [Rh(η^5-C_5Me_5)(H_2curc)(Cl)] × 2MeOH (**2**) with labels on rings. Displacement parameters are drawn at 50% probability level; solvent molecules are omitted for clarity.

The curcumin molecule is coordinated via its deprotonated acac oxygens (O1 and O2) forming a six-membered chelate ring with the Rh(III) ion. The metal-O distances and bite angles in these complexes are close to the values found in the analogous [Ru(η^6-*p*-cym)(acac)(Cl)] (2.074 Å, 88.0°) [36] and [Ru(η^6-*p*-cym)(H_2curc)(Cl)] [22] (2.071 Å, 87.4°) structures. These data show that acac is a good structural model of curcumin. On the other hand, the replacement of the arene moiety from *p*-cymene to toluene does not result in measurable effect on bond lengths and angles. The distance between the centre of gravity of the C_5Me_5 ring (ring A) and the Rh centre is 1.7485(15) Å, which falls within the range obtained for relevant Rh complexes (1.730-1.759 Å) [24,25,39-45]. In the complex with the heavier congener iridium ([Ir(η^5-C_5Me_5)(acac)(Cl)]) this distance is found to be 1.753 Å and the bite angle is 87.5°, which is slightly different. However, the metal-O distance is 2.100 Å, which is longer than in the Rh and Ru complexes [45].

Table 2. Selected bond distances (Å) and angles (°) of the metal complexes [Ru(η^6-tol)(acac)Cl] (**1**) and [Rh(η^5-C_5Me_5)(H_2curc)Cl] × 2MeOH (**2**) [a]

	[Ru(η^6-tol)(acac)Cl] (1)	**[Rh(η^5-C_5Me_5)(H_2curc)Cl] × 2MeOH (2)**
Bond lengths (Å)		
M—Cg[b]	1.415(10)	1.7485(15)
M—O1	2.073(4)	2.083(2)
M—O2	2.073(4)	2.073(2)
M—Cl	2.413(2)	2.4630(9)
Angles (°)		
O1—M—O2	88.2(2)	89.72(8)
O1—M—Cl	85.7(2)	87.08(7)
O2—M—Cl	84.4(1)	83.99(7)

[a] Uncertainties (SD) of the last digits are shown in parentheses.

[b] Cg is the centre of gravity calculated for different rings.

The two phenolic oxygens O3 and O5 remained protonated in [Rh(η^5-C_5Me_5)(H_2curc)Cl]. The curcumin molecule has a slightly bended conformation. The methoxy groups of the two 4-hydroxy-3-methoxyphenyl rings (ring C and D) are turned in opposite positions and the angle between the plain of the two rings is 15.32(15)°. The molecule is not symmetrically bended, ring B and C are almost in plane (the angle between their plains is 3.95(16)°), while higher angle could be measured between the plains of rings B and D (11.52(15)°). On Figure S7 different views of packing arrangement in crystal **2** are shown. Figure S8 shows the crystal-stabilizing hydrogen bond system and intermolecular distances are collected in Table S3.

Though the analogous Ru(II)-chlorido complex of curcumin was already crystallized [22], this is the first structure with its Rh(III) analogue. Figure 6 shows the comparison in the molecular conformations in crystal **2** with those of [Ru(η^6-cym)(H_2curc)(Cl)] × H_2O (Ref. code GESYAG) [22] and [Ru(η^6-cym)(dimethylH_2curc)(Cl)] × $CHCl_3$ × H_2O (Ref. code RESXUI) [46] where two molecules are in the asymmetric unit. It is clearly seen that the curcumin molecules can

adopt very different conformations and bending of the rings C and D can be even higher than in crystal **2** (see Table 3).

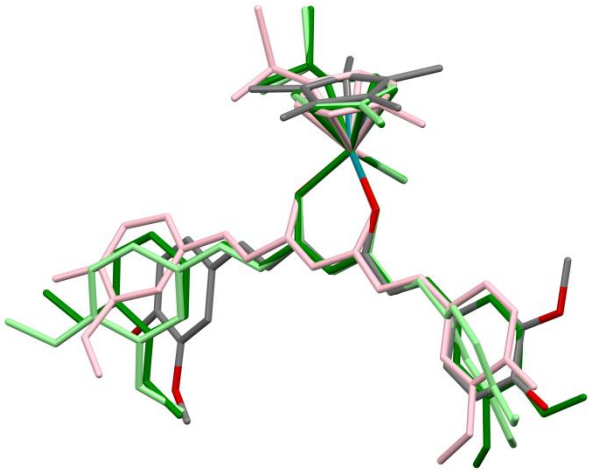

Figure 6. Comparison of molecular structure of [Rh(η^5-C_5Me_5)(H_2curc)(Cl)] (**2**) (coloured by element) with [Ru(η^6-cym)(H_2curc)(Cl)] (pink) (Ref. code GESYAG) [22] and the two molecules in the asymmetrical unit of [Ru(η^6-cym)(dimethylH_2curc)(Cl)] (dark and light green) (Ref. code RESXUI) [46]. Ru/Rh ions with the two oxygen and the chlorido ligands are superimposed.

Table 3. Comparison of the angles between curcumin ring planes in crystals [Rh(η^5-C_5Me_5)(H_2curc)(Cl)], [Ru(η^6-cym)(H_2curc)(Cl)] [22] and [Ru(η^6-cym)(dimethylH_2curc)(Cl)] [46].

	[Rh(η^5-C_5Me_5)(H_2curc)(Cl)]	**[Ru(η^6-cym)(H_2curc)(Cl)]**	**[Ru(η^6-cym)(dimethylH_2curc)(Cl)]**	
coloured	by element	pink	dark green	light green
AB (°)	67.8	51.7	66.0	69.2
BC (°)	4.0	8.1	11.8	47.5
BD (°)	11.5	13.2	14.7	38.5

2.5. H_2O/Cl^- exchange in [Rh(η^5-C_5Me_5)(acac)(H_2O)]$^+$

In the crystal structures of the studied half-sandwich organometallic complexes the coordination sphere of Ru(II) and Rh(III) contains the arene or arenyl group, the (O,O) donor bidentate and a chlorido ligand. While dissolving the complex in water, the good leaving group Cl^- can be substituted by a water molecule. It is considered as an important activation step according to the mechanism of action of similar complexes

[47], since the chlorido complex is suggested to be less reactive and charge neutral. Notably, the chloride ion concentration changes in biofluids: in the blood serum it is 100 mM, 23 mM in the cytoplasm and 4 mM in the nucleus [47]. The ratio of the aqua and chlorido complexes is changing as the compound reaches the nucleus from blood and this ratio is governed by the rate of the exchange process and log *K*' (H_2O/Cl^-) constant.

Based on the ^1H NMR spectra, in the case of Ru(η^6-*p*-cymene) and Ru(η^6-toluene) there is no pH range where only the acac complex is present in solution at 2 mM concentration. Therefore, this constant was determined only for the [Rh(η^5-C_5Me_5)(acac)(H_2O)]$^+$ complex at pH = 7.30 spectrophotometrically, using the same approach as in our previous works [24-29]. The water/chloride exchange was found to be fast, equilibrium could be reached within few minutes. In Figure 7 the spectral changes are clearly seen as the chloride ion concentration is increasing and the presence of one isobestic point proves the equilibrium between two species.

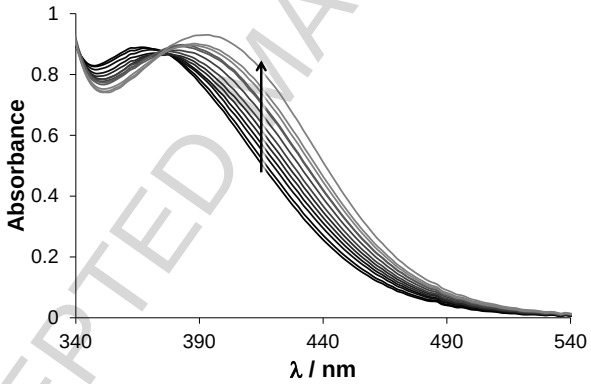

Figure 7. UV-Vis absorption spectra of [Rh(η^5-C_5Me_5)(acac)(H_2O)]$^+$ in the presence of chloride ions at different concentrations. {*c*([Rh(η^5-C_5Me_5)(H_2O)$_3$]$^{2+}$) = *c*(acac) = 1 mM; *c*(Cl^-) = 0 - 300 mM; pH = 7.30 (phosphate buffer); *T* = 25.0 °C}

The log *K*' (H_2O/Cl^-) constant is determined as 1.11 ± 0.03 (for fitting of the absorbance values see Figure S9), that reflects a moderate chloride ion affinity of the complex. Comparing this value to those of similar (O,O) donor bearing ligands' complexes *e.g.* maltol (1.17) [24], allomaltol (1.38) [24], deferiprone (0.78) [25], they are quite similar to each other, which means a relatively weak chloride ion affinity. Based on this constant it can be predicted that 56%, 23% and 5% is the fraction of the

chlorido species at 1 mM concentration of the complex and at physiological pH in blood serum, cytoplasm and nucleus, respectively.

2.6. In vitro cytotoxicity and interaction with proteins

Curcumin and its complexes were tested as anticancer compounds in a human colonic adenocarcinoma cell line Colo 320/MDR-LRP multidrug resistant overexpressing ABCB1 (MDR1)-LRP, using the thiazolyl blue tetrazolium bromide (MTT) method. Literature data reveal that [Ru(η^6-*p*-cym)(H_2curc)Cl] showed moderate cytotoxicity on HCT116 colon adenocarcinoma cell line (IC_{50} = 13.98 μM) [22]. [Rh(η^5-C_5Me_5)(H_2curc)Cl] possesses a similar activity as curcumin itself on A549 lung adenocarcinoma cells and the complex seems to be a delivery system of curcumin [23]. Herein the *in vitro* cytotoxicity studies of curcumin in the absence and in the presence of the various organometallic cations were carried out and IC_{50} values (after 24 h incubation) are collected in Table 4.

Table 4. *In vitro* cytotoxicity (IC_{50} values in mM in Colo 320 human colon cancer cell lines) of curcumin and its complexes (24 h exposure).

	IC_{50} (μM)
Curcumin + Ru(η^6-tol)(H_2O)$_3$]$^{2+}$	82.3 ± 1.5
Curcumin + Ru(η^6-*p*-cym)(H_2O)$_3$]$^{2+}$	63.1 ± 3.6
Curcumin + Rh(η^5-C_5Me_5)(H_2O)$_3$]$^{2+}$	34.8 ± 0.2
Curcumin	39.6 ± 2.4

Data reveal that curcumin and its premixed Rh(η^5-C_5Me_5) complex have similar cytotoxic effect, while for the premixed organoruthenium complexes lower bioactivity was determined. Based on these values the free curcumin is effective alone, while complexation with [Rh(η^5-C_5Me_5)(H_2O)$_3$]$^{2+}$ does not disturb this effect, although complex formation with [Ru(η^6-*p*-cymene)(H_2O)$_3$]$^{2+}$ and [Ru(η^6-toluene)(H_2O)$_3$]$^{2+}$ interferes with it. To understand better the findings of the *in vitro* cytotoxic measurements the effect of the cell culture medium components on complex stability was studied. Cancer cells were grown in a cell culture medium RPMI 1640

supplemented with 10% heat-inactivated fetal bovine serum (FBS) and 100 mM HEPES. This modified medium contains different inorganic salts, amino acids and some other small biomolecules, e.g. folic acid and choline chloride from RPMI 1640 and various serum proteins from FBS. The serum components have effects on stability of both curcumin and its complex, since the hydrolytic stability of curcumin is increasing [19,20], however the coordination of amino acid side chains can cause decomposition of the original metal complex [28]. Interaction of $[Rh(\eta^5\text{-}C_5Me_5)(acac)(H_2O)]^+$ and RPMI 1640 components with and without FBS was monitored by ^1H NMR spectroscopy (Figure 8).

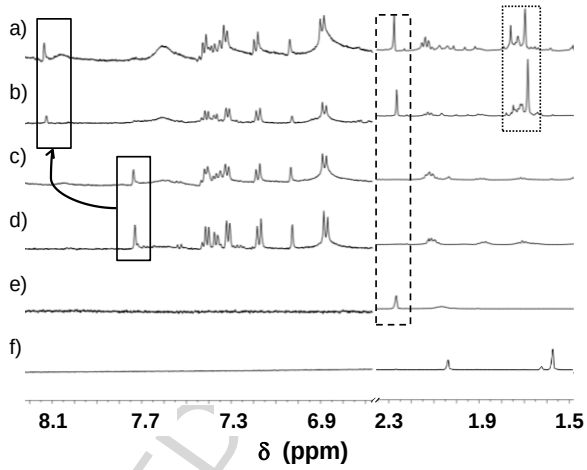

Figure 8. ^1H NMR spectra recorded for $[Rh(\eta^5\text{-}C_5Me_5)(acac)(H_2O)]^+$ in RPMI 1640 and RPMI 1640 with 10% FBS media. a) $[Rh(\eta^5\text{-}C_5Me_5)(acac)(H_2O)]^+$ in RPMI 1640 with 10% FBS medium; b) $[Rh(\eta^5\text{-}C_5Me_5)(acac)(H_2O)]^+$ in RPMI 1640 medium; c) RPMI 1640 with 10% FBS medium; d) RPMI 1640 medium; e) free acac in buffered solution at pH = 7.4 (PBS'); f) $[Rh(\eta^5\text{-}C_5Me_5)(acac)(H_2O)]^+$ in buffered solution at pH = 7.4 (PBS'). Dotted rectangle: C_5Me_5 protons at various binding environment; dashed rectangle: free acac methyl groups; solid rectangles: His proton. {$c([Rh(\eta^5\text{-}C_5Me_5)(acac)(H_2O)]^+) = c(acac) = 1$ mM; solvent: 90% H_2O / 10% D_2O; $T = 25.0$ °C; $t = 24$ h}

The chloride ion content of this medium is ~110 mM, which means that around 56% of the complex is chlorinated on the basis of the determined log K' (H_2O/Cl^-) constant. The recorded ^1H NMR spectra show that the complex dissociates in both media: free acac is detected and the organometallic rhodium cation is in different environments, most probably His is bound to it. In the FBS modified medium different peaks are seen which indicates protein-rhodium interactions. In the case of the organoruthenium

cations complex decomposition can be detected, but there is no difference in the binding environment in the two types of medium (Figures S10 and S11).

Human serum albumin (HSA) is the main transport protein in blood and considered as an useful model protein to examine the protein – metal complex interactions. It can bind drug molecules in its binding pockets non-specifically and metal ions and complexes through coordinating side chains. Using spectrofluorimetry binding close to binding site I (IIA subdomain) can be monitored, as Trp-214 is sensitive to the binding in this pocket and it can be selectively excited. The binding of curcumin to HSA was already investigated several times by other groups and with different methods [48,49]. The binding constant is determined as log K = 5.79 by spectrofluorimetry and one curcumin molecule binds to one HSA molecule [50].

Binding of $[Rh(\eta^5\text{-}C_5Me_5)(H_2O)_3]^{2+}$ and $[Ru(\eta^6\text{-tol})(H_2O)_3]^{2+}$ towards HSA was characterized previously in our research group [28,29]. The interaction of HSA and $[Ru(\eta^6\text{-}p\text{-cym})(H_2O)_3]^{2+}$ has the same characteristics as in the two other cases. Quenching constant (log K'_Q) can be calculated based on the emission changes of Trp-214. In the case of $[Ru(\eta^6\text{-}p\text{-cym})(H_2O)_3]^{2+}$ this value is 5.60 ± 0.01. HSA has high metal ion affinity, because it can bind at least 8-fold excess of these cations [28,29]. Based on spectrofluorimetric and ultrafiltration experiments the binding of acac to HSA was excluded.

In our experimental setup 1 μM of HSA was titrated with the organometallic ions and with their acac complexes from 1:1 up to 1:10 HSA-to-metal ion/or complex ratio and emission spectra were recorded upon excitation at 295 nm after 24 h waiting time. Figure 9 shows the spectral changes as the function of HSA-to-metal ion/complex ratio in case of the $Ru(\eta^6\text{-}p\text{-cym})$ species as representative example. The presence of acac results in negligible difference.

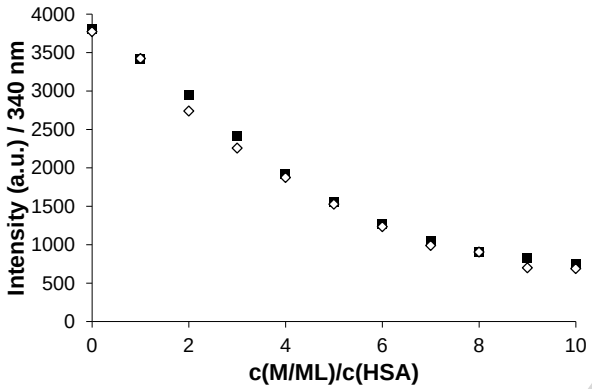

Figure 9. Fluorescence emission intensity at 340 nm of the HSA – $[Ru(\eta^6\text{-}p\text{-cym})(H_2O)_3]^{2+}$ (◊) and the HSA – $[Ru(\eta^6\text{-}p\text{-cym})(acac)(H_2O)]^{+}$ (■) systems. {λ_{EX} = 295 nm; c(HSA) = 1 μM; c([$Ru(\eta^6$-tol)$(H_2O)_3]^{2+}$) = c(acac) = 0-10 μM; T = 25.0 °C; pH = 7.4 (PBS' buffer); t = 24 h}

Then ultrafiltration/UV-Vis measurements were performed to reveal in which form the acac complexes bind to the protein. We found that free acac appears in the filtrate (see Figure S12.) with only a very small amount of complex. Therefore, most of the organometallic ions are bound to the protein and the ligand is cleaved, so they exhibit a dissociative binding mode.

3. Conclusions

Curcumin and organometallic half-sandwich complexes are in the focus of attention since their anticancer activity is widely reported. The half-sandwich curcumin complexes are very attractive drug candidates but limited data are reported about their stability in aqueous solution and in biological media. In this work we determined the pK_a values of curcumin and stability constants of the curcumin complex of $[Rh(\eta^5\text{-}C_5Me_5)(H_2O)_3]^{2+}$ with UV-Vis spectroscopy in aqueous solution and in dark. It was found that acetylacetone is not a perfect but still a good binding model for curcumin based on the determined stability constants, since $[Rh(\eta^5\text{-}C_5Me_5)(H_2curc)(H_2O)]^{+}$ shows only a bit higher stability than $[Rh(\eta^5\text{-}C_5Me_5)(acac)(H_2O)]^{+}$. These complexes possess lower stability than other half-sandwich Rh and Ru complexes formed with (O,O) bidentate ligands. The trend of the stability constant (log K [ML]) values determined is $Ru(\eta^6\text{-}p\text{-cymene}) > Ru(\eta^6\text{-toluene}) > Rh(\eta^5\text{-}C_5Me_5)$, however due to the highest hydrolytic stability of $[Rh(\eta^5\text{-}C_5Me_5)(H_2O)_3]^{2+}$ cation, at physiological pH the $Rh(\eta^5\text{-}C_5Me_5)$ complex is formed at the highest extent. In the basic pH range, decomposition of metal complexes to $[M_2(OH)_3]^{+}$ is observed and formation of mixed

hydroxido complex [[Ru(η^6-tol)(acac)(OH)] is detected. The water/chlorido exchange constant provides information about the ratio of aqua and chlorido complexes in different biological media at physiological pH. 56%, 23% and 5% were found to be the ratio of the chlorido complex in blood serum, cytoplasm and nucleus, respectively at 1 mM concentration of the [Rh(η^5-C_5Me_5)-acac complex.

The *in vitro* cytotoxicity tests in a multidrug resistant human colonic adenocarcinoma cell line revealed that only the complex [Rh(η^5-C_5Me_5)(H_2curc)(H_2O)]$^+$ shows similar anticancer activity compared to that of curcumin, the [Ru(η^6-arene)(H_2O)$_3$]$^{2+}$ cations decrease this effect. It was also found that the interaction of these complexes with cell culture medium components and serum proteins results in decomposition of complexes. ^{1}H NMR spectra indicate that the organometallic fragment is bound to amino acids and proteins. Upon the interaction with the model protein HSA decomposition of metal complexes and metal binding via the release of the ligand was detected.

4. Experimental

4.1. Chemicals

All solvents were of analytical grade and used without further purification. [Rh(η^5-C_5Me_5)(μ^2-Cl)Cl]$_2$, [Ru(η^6-*p*-cym)(μ^2-Cl)Cl]$_2$, curcumin (≥99.5%), acetylacetone, maltol, deferiprone, $RuCl_3 \times 3H_2O$, KCl, $AgNO_3$, HCl, KOH, 4,4-dimethyl-4-silapentane-1-sulfonic acid (DSS), HSA (as lyophilized powder with fatty acids, A1653), RPMI 1640, NaH_2PO_4, Na_2HPO_4, KH_2PO_4, toluene, ethanol and methanol were purchased from Sigma-Aldrich in puriss quality. Doubly distilled Milli-Q water was used for sample preparation. The dimeric ruthenium precursor [Ru(II)(η^6-tol)(μ^2-Cl)Cl]$_2$ was prepared according to literature procedures [38]. The exact concentration of the ligand stock solutions together with the proton dissociation constants were determined by pH-potentiometric titrations with the use of the computer program HYPERQUAD [51]. The aqueous [Rh(η^5-C_5Me_5)(H_2O)$_3$](NO_3)$_2$ stock solution was obtained by dissolving an exact amount of the dimeric precursor in water followed by the removal of chloride ions by addition of equivalent amounts of $AgNO_3$. The exact concentrations of chloride ion containing and chloride free metal ion stock solutions were determined by pH-potentiometric titrations employing stability constants for [(Rh(η^5-

$C_5Me_5))_2(\mu^2\text{-}OH)_i]^{(4-i)+}$, $[(Ru(\eta^6\text{-tol}))_2(\mu^2\text{-}OH)_i]^{(4-i)+}$ and $[(Ru(\eta^6\text{-}p\text{-cym}))_2(\mu^2\text{-}OH)_i]^{(4-i)+}$ (i = 2 or 3) complexes [24,30].

The stock solution of curcumin was prepared prior to the analysis on a weight-in-volume basis dissolved in ethanol and kept in dark. HSA solution was freshly prepared before the experiments and its concentration was estimated from its UV absorption: $\varepsilon_{280\ nm}$(HSA) = 36850 $M^{-1}cm^{-1}$ [52]. It was dissolved in a modified phosphate buffered saline (PBS') at pH 7.40. PBS' contains 12 mM Na_2HPO_4, 3 mM KH_2PO_4, 1.5 mM KCl and 100.5 mM NaCl; and the concentration of the K^+, Na^+ and Cl^- ions corresponds to that of the human blood serum.

4.2. Synthesis of the precursor [Ru(η⁶-tol)(μ²-Cl)Cl]₂

$[Ru(\eta^6\text{-tol})(\mu^2\text{-Cl})Cl]_2$ was prepared according the literature procedure used for the analogous $[Ru(\eta^6\text{-benzene})(\mu^2\text{-Cl})Cl]_2$ [38] by adding 5 mL of 1-methyl-1,4-cyclohexadiene to a solution of 0.5 g $RuCl_3 \times 3H_2O$ (1.9 mmol) in 40 mL of absolute ethanol. This mixture was refluxed for 8 h. The reddish brown precipitate formed during the synthesis was filtered off, washed with diethyl ether and left to dry in exsiccator. Yield: 85%, 0.450 g; ^{1}H NMR (500.26 MHz, DMSO-d_6, δ, ppm): 2.12 (3H, s, CH_3), 5.68 (3H, m, C2, C4, C6 toluene), 5.97 (2H, m, C3, C5 toluene); ^{13}C NMR (125.79 MHz, DMSO-d_6, δ, ppm) 18.73 (CH_3), 82.22 (C4 toluene), 84.83 (C5, C3 toluene), 89.28 (C6, C2 toluene), 105.82 (C1 toluene).

4.3. Crystallographic structure determination

Single crystals suitable for X-ray diffraction experiment of compounds $[Ru(\eta^6\text{-tol})(acac)(Cl)]$ (**1**), and $[Rh(\eta^5\text{-}C_5Me_5)(H_2curc)(Cl)] \times 2MeOH$ (**2**) were grown from MeOH or CH_2Cl_2/MeOH solution resulting in yellow and red single crystals, respectively. They were mounted on a loop and transferred to the goniometer. X-ray diffraction data were collected at -170 °C on a Rigaku RAXIS-RAPID II diffractometer using Mo-K_α radiation for crystal **1** and Cu-K_α for crystal **2**. A numerical absorption correction [53] was carried out in case of crystal **1** and a multi-scan absorption correction was used in case of crystal **2** using the software CrystalClear [54]. Sir2014 [55] and SHELXL [56] under WinGX [57] softwares were used for structure solution and refinement, respectively. The structures were solved by direct methods. The models were refined by full-matrix least squares on F^2. Refinement of non-hydrogen atoms was carried out with anisotropic temperature factors. Hydrogen atoms were placed into geometric positions. They were included in structure factor calculations but they were not refined. The isotropic displacement parameters of the hydrogen atoms were

approximated from the U(eq) value of the atom they were bonded to. The summary of data collection and refinement parameters are collected in Table S1. Selected bond lengths and angles of compounds were calculated by PLATON software [58]. The graphical representation and the edition of CIF files were done by Mercury [59] and PublCif [60] softwares, respectively. The crystallographic data files for the complexes have been deposited with the Cambridge Crystallographic Database as CCDC 1882689 and 1882690.

4.4. pH-Potentiometric measurements

pH-Potentiometric measurements determining proton dissociation constants of ligands and overall stability constants for the metal complexes were carried out at 25.0 ± 0.1 °C in water and at a constant ionic strength of 0.20 M KCl. The titrations were performed in a carbonate-free KOH solution (0.20 M). The exact concentrations of HCl and KOH solutions were determined by pH-potentiometric titrations. An Orion 710A pH-meter equipped with a Metrohm combined electrode (type 6.0234.100) and a Metrohm 665 Dosimat burette were used for the pH-potentiometric measurements. The electrode system was calibrated to the pH = −log[H^+] scale by means of blank titrations (HCl vs. KOH), as suggested by Irving *et al.* [61]. The average water ionization constant, pK_w, was determined as 13.76 ± 0.01 at 25.0 °C, I = 0.20 M (KCl), which is in accordance to literature [62]. The reproducibility of the titration points included in the calculations was within 0.005 pH units. The pH-potentiometric titrations were performed in the pH range between 2.0 and 11.5. The initial volume of the samples was 5.0 mL. The ligand concentration was 2.0 mM and was investigated at metal ion-to-ligand ratios of 1:1, 1:1.5, and 1:2. The accepted fitting between the measured and calculated titration data points regarding the volume of the titrant was < 10 μL. Samples were degassed by bubbling purified argon through them for about 10 minutes prior to the measurements and the inert gas was also passed over the solutions during the titrations.

The computer program PSEQUAD [63] was utilized to establish the stoichiometry of the complexes and to calculate the overall stability constants. $\beta(M_pL_qH_r)$ is defined for the general equilibrium:

$$pM + qL + rH \rightleftharpoons M_pL_qH_r; \text{ as } \beta(M_pL_qH_r) = [M_pL_qH_r]/([M]_p[L]_q[H]_r)$$

where M denotes the metal moiety $[Rh(\eta^5\text{-}C_5Me_5)(H_2O)_3]^{2+}$ or $[Ru(\eta^6\text{-arene})(H_2O)_3]^{2+}$ and L the completely deprotonated ligand. β values for the various hydroxido complexes [(Rh(η^5-

$C_5Me_5))_2(\mu^2\text{-}OH)_i]^{(4-i)+}$, $[(Ru(\eta^6\text{-tol}))_2(\mu^2\text{-}OH)_i]^{(4-i)+}$ and $[(Ru(\eta^6\text{-}p\text{-cym}))_2(\mu^2\text{-}OH)_i]^{(4-i)+}$ (i = 2 or 3) were calculated based on the pH-potentiometric titration data and were found to be in good agreement with the previously published data [24,30].

4.5. UV-Vis spectrophotometric and ^{1}H NMR measurements

A Hewlett Packard 8452A diode array spectrophotometer was used to record the UV-Vis spectra in the interval 200–800 nm. The path length (*l*) was 0.5, 1, or 2 cm. The proton dissociation constants of curcumin were determined spectrophotometrically by batch method to avoid the photodegradation. Samples contained 5 μM curcumin and 5% (v/v) ethanol. UV-Vis spectra were used to investigate the H_2O/Cl^- exchange processes of complexes at 1 mM concentration, at pH 7.30 (20 mM phosphate buffer) as a function of chloride concentrations (0–300 mM).

^{1}H NMR studies were carried out on a Bruker Avance III HD 500 MHz instrument. All ^{1}H NMR spectra were recorded with the WATERGATE water suppression pulse scheme using DSS internal standard. Acetylacetonate was dissolved in a 10% (v/v) D_2O/H_2O mixture to yield a concentration of 2 mM and was titrated at 25 °C, at I = 0.20 M (KCl) in absence or presence of $[Rh(\eta^5\text{-}C_5Me_5)(H_2O)_3]^{2+}$ and $[Ru(\eta^6\text{-tol})(H_2O)_3]^{2+}$ at 1:1 metal-to-ligand ratio. Stability constants for the complexes were calculated by the computer program PSEQUAD [63].

4.6. Fluorescence and membrane ultrafiltration/UV-Vis studies with HSA

Fluorescence spectra were recorded on a Hitachi-F4500 fluorimeter in 1 cm quartz cell at 25.0 ± 0.1 °C. All solutions were prepared in PBS' (pH 7.40) and were incubated for 15 min or 24 h. Samples contained 1 μM HSA and various HSA-to-ligand or metal ion or metal complex ratios (from 1:0 to 1:10) were used. The excitation wavelength was 295 nm and the emission was read in the range of 305-450 nm. The quenching constant (log K'_Q) was calculated with the computer program PSEQUAD [63] using the same approach applied in our previous works [28,29].

Samples were separated by ultrafiltration through 10 kDa membrane filters (Microcon YM-10 centrifugal filter unit, Millipore) in low (LMM) and high molecular mass (HMM) fractions with the help of a temperature controlled centrifuge (Sanyo, 10000/s, 10 min). Samples (0.50 mL) contained 50 μM HSA and $Rh(\eta^5\text{-}C_5Me_5)$ or its acac complex (150 μM) in PBS' buffer (pH 7.30) at 25.0 ± 0.1 °C and were incubated for 24 h. The LMM fraction

containing the non-bound metal complex was separated from the protein and its adducts in the HMM fraction. The concentration of the non-bound compounds in the LMM fractions was determined by UV-Vis spectrophotometry by comparing the recorded spectra to those of reference samples without the protein. When the complex decomposed due to the protein binding, free ligand was also detected in the LMM fraction. In this case the recorded spectra were deconvoluted using the molar absorbance spectra of the ligand and metal complex by Excel Solver (Microsoft Office 2007).

4.7. Cell lines, culture conditions and cytotoxicity tests in cancer cell lines

Cell lines and culture conditions: All cell culture reagents were obtained from Sigma-Aldrich and plastic ware from Sarstedt (Germany). Human colonic adenocarcinoma cell line Colo 320/MDR-LRP multidrug resistant overexpressing ABCB1 (MDR1)-LRP (ATCC-CCL-220.1) was purchased from LGC Promochem, Teddington, UK. The cells were cultured in RPMI 1640 medium supplemented with 10% heat-inactivated fetal bovine serum, 2 mM L-glutamine, 1 mM sodium pyruvate and 100 mM 4-(2-hydroxyethyl)-1-piperazineethanesulfonic acid (HEPES). The cells were incubated at 37 °C, in a 5% CO_2, 95% air atmosphere. The semi-adherent human colon cancer cells were detached with Trypsin-Versene (EDTA) solution for 5 min at 37 °C.

MTT assay: Curcumin and its premixed Rh(η^5-C_5Me_5) and Ru(η^6-arene) complexes were dissolved in an ethanol/PBS' (1:1) mixture first, diluted in complete culture medium, then two-fold serial dilutions of compounds were prepared in 100 μL of RPMI 1640, horizontally. The semi-adherent colonic adenocarcinoma cells were treated with Trypsin-Versene (EDTA) solution. They were adjusted to a density of 1×10^4 cells in 100 μL of RPMI 1640 medium, and were added to each well, with the exception of the medium control wells. The final volume of the wells containing compounds and cells was 200 μL.

The culture plates were incubated at 37˚C for 24 h; at the end of the incubation period, 20 μL of MTT (Sigma) solution (from a stock solution of 5 mg/mL) were added to each well. After incubation at 37˚C for 4 h, 100 μL of sodium dodecyl sulfate (SDS) (Sigma) solution (10% in 0.01 M HCI) were added to each well and the plates were further incubated at 37˚C overnight. Cell growth was determined by measuring the optical density (OD) at 540/630 nm with Multiscan EX ELISA reader (Thermo Labsystems, Cheshire, WA, USA). Inhibition of the cell growth (IC_{50}) was determined according to the formula below:

$$100-\left[\frac{OD_{\text{sample}}-OD_{\text{medium control}}}{OD_{\text{cell control}}-OD_{\text{medium control}}}\right]\times 100$$

Acknowledgements

This work was supported by National Research, Development and Innovation Office-NKFIA through projects GINOP-2.3.2-15-2016-00038, FK 124240, K 115762, Ministry of Human Capacities, Hungary grant 20391-3/2018/FEKUSTRAT and the J. Bolyai Research Scholarship of the Hungarian Academy of Sciences (É.A.E, N.V.M.). The authors thank Ms. Fanni Veréb for performing some titrations.

References

[1] V. Brabec, O. Hrabina, J. Kasparkova, Coord. Chem. Rev. 351 (2017) 2–31. doi: 10.1016/j.ccr.2017.04.013

[2] M.A. Jakupec, M. Galanski, V.B. Arion, C.G. Hartinger, B.K. Keppler, Dalton Trans. (2008) 183–194. doi: 10.1039/B712656P

[3] E. Alessio, Eur. J. Inorg. Chem. 12 (2017) 1549–1560. doi: 10.1002/ejic.201600986

[4] R. Trondl, P. Heffeter, C.R. Kowol, M.A. Jakupec, W. Berger, B.K. Keppler, Chem. Sci. 5 (2014) 2925–2932. doi: 10.1039/C3SC53243G

[5] H.A. Burris, S. Bakewell, J.C. Bendell, J. Infante, S. Jones, D.R. Spigel, G.J. Weiss, R.K. Ramanathan, A. Ogden D. Von Hoff, ESMO Open 1 (2017) e000154. doi: 10.1136/esmoopen-2016-000154

[6] https://clinicaltrials.gov/ct2/show/NCT03053635 (accessed on 20th December 2018)

[7] Y. Geldmacher, M. Oleszak, W.S. Sheldrick, Inorg. Chim. Acta 393 (2012) 84–102. doi: 10.1016/j.ica.2012.06.046

[8] B. Therrien, Coord. Chem. Rev. 253 (2009) 493–519. doi: 10.1016/j.ccr.2008.04.014

[9] B.S. Murray, M.V. Babak, C.G. Hartinger, P.J. Dyson, Coord. Chem. Rev. 306 (2016) 86–114. doi: 10.1016/j.ccr.2015.06.014

[10] H.-K. Liu, P.J. Sadler, Acc. Chem. Res. 44 (2011) 349–359. doi: 10.1021/ar100140e

[11] P. Zhang, P.J. Sadler, J. Organomet. Chem. 839 (2017) 5–14. doi: 10.1016/j.jorganchem.2017.03.038

[12] S.H. van Rijt, A.F.A. Peacock, P.J. Sadler in Platinum and Other Heavy Metal Compounds in Cancer Chemotherapy, (Eds.: A. Bonetti, R. Leone, F. M. Muggia, S. B. Howell), Humana Press, Totowa, NJ, 2009, pp. 73–79. doi: 10.1007/978-1-60327-459-3

[13] R. Pettinari, F. Marchetti, C. Di Nicola, C. Pettinari, Eur. J. Inorg. Chem. 31 (2018) 3521–3536. doi: 10.1002/ejic.201800400

[14] A. Petrini, R. Pettinari, F. Marchetti, C. Pettinari, B. Therrien, A. Galindo, R. Scopelliti, T. Riedel, P.J. Dyson, Inorg. Chem. 56 (2017) 13600–13612. doi: 10.1021/acs.inorgchem.7b02356

[15] T. Nabekura, Toxins 2 (2010) 1207–1224. doi: 10.3390/toxins2061207

[16] K.M. Nelson, J.L. Dahlin, J. Bisson, J. Graham, G.F. Pauli, M.A. Walters, J. Med. Chem. 60 (2017) 1620–1637. doi: 10.1021/acs.jmedchem.6b00975

[17] D. Lee, I.Y. Kim, S. Saha, K.S. Choi, Pharmacol. Ther. 162 (2016) 120–133. doi:

[18] S. Mondal, S. Ghosh, S.P. Moulik, J. Photochem. Photobiol. B, Biol. 158 (2016) 212–218. doi: 10.1016/j.pharmthera.2016.01.003

[19] M.H.M. Leung, T.W. Kee, Langmuir 25 (2009) 5773–5777. doi: 10.1021/la804215v

[20] Y.-J. Wang, M.-H. Pan, A.-L. Cheng, L.-I. Lin, Y.-S. Ho, C.-Y. Hsieh, J.-K. Lin, J. Pharm. Biomed. Anal. 15 (1997) 1867–1876. doi: 10.1016/S0731-7085(96)02024-9

[21] S. Banerjee, A.R. Chakravarty, Acc. Chem Res. 48 (2015) 2017–2083. doi: 10.1021/acs.accounts.5b00127

[22] F. Caruso, M. Rossi, A. Benson, C. Opazo, D. Freedman, E. Monti, M.B. Gariboldi, J. Shaulky, F. Marchetti, R. Pettinari, C. Pettinari, J. Med. Chem. 55 (2012) 1072–1081. doi: 10.1021/jm200912j

[23] J. Markham, J. Liang, A. Levina, R. Mak, B. Johannessen, P. Kappen, C.J. Glover, B. Lai, S. Vogt, P.A. Lay, Eur. J. Inorg. Chem. 2017 (2017) 1812–1823. doi: 10.1002/ejic.201601331

[24] O. Dömötör, S. Aicher, M. Schmidlehner, M.S. Novak, A. Roller, M.A. Jakupec, W. Kandioller, C.G. Hartinger, B.K. Keppler, É.A. Enyedy, J. Inorg. Biochem. 134 (2014) 57–65. doi: 10.1016/j.jinorgbio.2014.01.020

[25] É.A. Enyedy, O. Dömötör, C.M. Hackl, A. Roller, M.S. Novak, M.A. Jakupec, B.K. Keppler, W. Kandioller, J. Coord. Chem. 68 (2015) 1583–1601. doi: 10.1080/00958972.2015.1023195

[26] O. Dömötör, V.F.S. Pape, N.V. May, G. Szakács, É.A. Enyedy, Dalton Trans. 46 (2017) 4382–4396. doi: 10.1039/C7DT00439G

[27] J. P. Mészáros, O. Dömötör, C. M. Hackl, A. Roller, B. K. Keppler, W. Kandioller, É. A. Enyedy, New J. Chem. 42 (2018) 11174–11184. doi: 10.1039/C8NJ01681J

[28] É.A. Enyedy, J.P. Mészáros, O. Dömötör, C.M. Hackl, A. Roller, B.K. Keppler, W. Kandioller, J. Inorg. Biochem. 152 (2015) 93–103. doi:

[29] J.M. Poljarević, G.T. Gál, N.V. May, G. Spengler, O. Dömötör, A.R. Savić, S. Grgurić-Šipka, É.A. Enyedy, J. Inorg. Biochem. 181 (2018) 74–85. doi: 10.1016/j.jinorgbio.2015.08.025

[30] L. Bíró, A.J. Godó, Z. Bihari, E. Garribba, P. Buglyó, Eur. J. Inorg. Chem. 2013 (2013) 3090–3100. doi: 10.1002/ejic.201201527

[31] L. Bíró, E. Farkas, P. Buglyó, Dalton Trans. 41 (2012) 285–291. doi: 10.1039/C1DT11405K

[32] J. Bunting, J. Kanter, R. Nelander, Z. Wu, Can. J. Chem. 73 (1995) 1305–1311. doi: 10.1139/v95-161

[33] M. Borsari, E. Ferrari, R. Grandi, M. Saladini, Inorg. Chim. Acta 328 (2002) 61-68. doi: 10.1016/S0020-1693(01)00687-9

[34] M. Bernabé-Pineda, M.T. Ramírez-Silva, M. Romero-Romo, E. González-Vergara, A. Rojas-Hernández, Spectrochim. Acta, Part A 60 (2004) 1091–1097. doi: 10.1016/S1386-1425(03)00342-1

[35] L. Bíró, E. Farkas, P. Buglyó, Dalton Trans. 39 (2010) 10272–10278. doi: 10.1039/C0DT00469C

[36] R. Fernández, M. Melchart, A. Habtemariam, S. Parsons, P.J. Sadler, Chem. Eur. J. 10 (2004) 5173–5179. doi: 10.1002/chem.200400640

[37] K.N. Raymond, C.J. Carrano, Acc. Chem. Res. 12 (1979) 183–190. doi: 10.1021/ar50137a004

[38] R.A. Zelonka, M.C. Baird, Can. J. Chem. 50 (1972) 3063–3072. doi: 10.1139/v72-486

[39] A.P. Abbott, G. Capper, D.L. Davies, J. Fawcett, D.R. Russell, J. Chem. Soc., Dalton Trans. (1995) 3709–3713. doi: 10.1039/DT9950003709

[40] F.-N. Ng, Y.-F. Lau, Z. Zhou, W.-Y. Yu, Org. Lett. 17 (2015) 1676–1679. doi: 10.1021/acs.orglett.5b00440

[41] P. Govindaswamy, D. Linder, J. Lacour, G. Süss-Fink, B. Therrien, Dalton Trans. (2007) 4457–4463. doi: 10.1039/b709247d

[42] Y.-F. Han, Y.-J. Lin, W.-G. Jia, L.-H. Weng, G.-X. Jin, Organometallics 26 (2007) 5848–5853. doi: 10.1021/om700691u

[43] W.H. Ang, Z. Grote, R. Scopelliti, L. Juillerat-Jeanneret, K. Severin, P.J. Dyson, J. Organomet. Chem. 694 (2009) 968–972. doi: 10.1016/j.jorganchem.2008.11.026

[44] C. Pettinari, R. Pettinari, M. Fianchini, F. Marchetti, B.W. Skelton, A.H. White Inorg.Chem. 44 (2005) 7933–7942. doi: 10.1021/ic050985r

[45] C.M. DuChane, L.C. Brown, V.S. Dozier, J.S. Merola, Organometallics 37 (2018) 530–538. doi: 10.1021/acs.organomet.7b00742

[46] F. Kühlwein, K. Polborn, W. Beck, Z. Anorg. Allg. Chem. 623 (1997) 1211–1219. doi: 10.1002/zaac.19976230806

[47] A.M. Pizarro, A. Habtemariam, P.J. Sadler, Top. Organomet. Chem. 32 (2010) 21–56. doi: 10.1007/978-3-642-13185-1_2

[48] F. Zsila, Z. Bikádi, M. Simonyi, Biochem. Biophys. Res. Commun. 301 (2003) 776–782. doi: 10.1016/S0006-291X(03)00030-5

[49] Y.S. Ge, C. Jin, Z. Song, J.-Q. Zhang, F.-L. Jiang, Y. Liu, Spectrochim. Acta, Part A 124 (2014) 265–276. doi: 10.1016/j.saa.2014.01.009

[50] M. Maciążek-Jurczyk, M. Maliszewska, J. Pożycka, J. Równicka-Zubik, A. Góra, A. Sułkowska, J. Mol. Struct. 1044 (2013) 194–200. doi: 10.1016/j.molstruc.2012.11.024

[51] P. Gans, A. Sabatini, A. Vacca, Talanta 43 (1996) 1739–1753. doi: 10.1016/0039-9140(96)01958-3

[52] G.H. Beaven, S. Chen, A. D'Albis, W. B. Gratzer, Eur. J. Biochem. 42 (1974) 539–546. doi: 10.1111/j.1432-1033.1974.tb03295.x

[53] T. Higashi, NUMABS. Rigaku/MSC Inc., Tokyo, Japan, 2002

[54] CrystalClear. Rigaku/MSC Inc., Tokyo, Japan, 2008

[55] M.C. Burla, R. Caliandro, B. Carrozzini, G.L. Cascarano, C. Cuocci, C. Giacovazzo, M. Mallamo, A. Mazzone, G. Polidori, J. Appl. Crystallogr. 48 (2015) 306–309. doi: 10.1107/S1600576715001132

[56] SHELXL-2013 Program for Crystal Structure Solution, University of Göttingen, Germany, 2013

[57] L.J. Farrugia, J. Appl. Crystallogr. 45 (2012) 849–854. doi: 10.1107/S0021889812029111

[58] A.L. Spek, J. Appl. Crystallogr. 36 (2003) 7–13. doi: 10.1107/S0021889802022112

[59] C.F. Macrae, P.R. Edgington, P. McCabe, E. Pidcock, G.P. Shields, R. Taylor, M. Towler, J. van De Streek, J. Appl. Crystallogr. 39 (2006) 453–457. doi: 10.1107/S002188980600731X

[60] S.P. Westrip, J. Appl. Crystallogr. 43 (2010) 920–925. doi: 10.1107/S0021889810022120

[61] H.M. Irving, M.G. Miles, L.D. Petit, Anal. Chim. Acta 38 (1967) 475–482. doi: 10.1016/S0003-2670(01)80616-4

[62] SCQuery, The IUPAC Stability Constants Database, Academic Software (Version 5.5), R. Soc. Chem., 1993–2005.

[63] L. Zékány, I. Nagypál in Computational Methods for the Determination of Stability Constants (Ed.: D. L. Leggett), Plenum Press, New York, 1985, pp. 291–353.

Synopsis

Solution stability of Ru(II)(η^6-toluene), Ru(II)(η^6-*p*-cymene) and Rh(III)(η^5-C_5Me_5) complexes of acetylacetone was determined in aqueous solution and compared with that of other (O,O) donor ligands. The structures of [Rh(III)(η^5-C_5Me_5)(H_2curcumin)]$^+$ and [Ru(II)(η^5-toluene)(acac)]$^+$ were resolved by single crystal X-ray diffraction. Their cytotoxicity was evaluated in multidrug resistant human cancer cell lines.

Graphical abstract

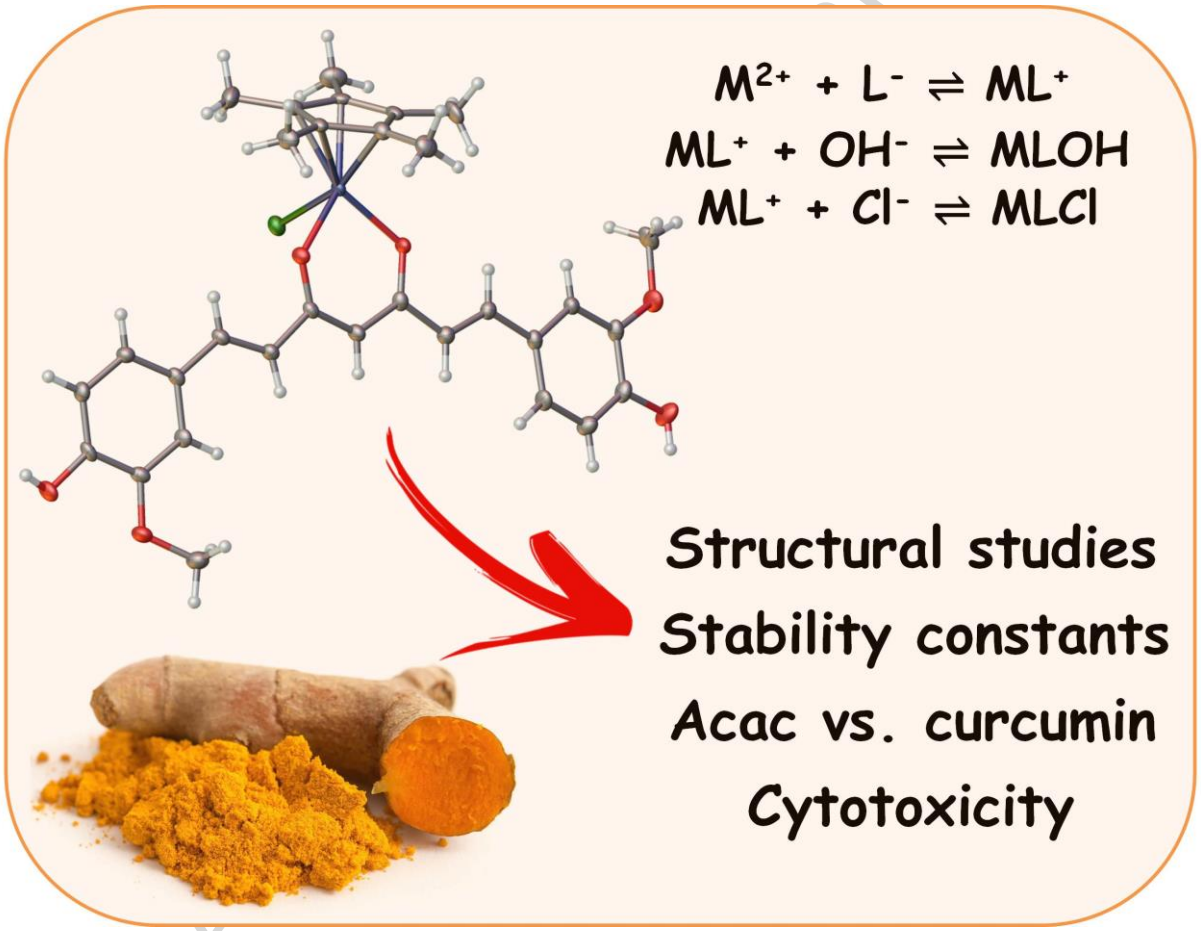

Highlights

- ► Solution stability of Ru(arene) and Rh(C_5Me_5) complexes of acac and curcumin
- ► Acac is used as curcumin binding model
- ► X-ray crystal structures of two complexes and comparison with analogous structures
- ► Antiproliferative activity against multidrug resistant human cancer cell lines
- ► Human serum albumin binding and interaction with cell culture medium components